



TOPOLOGICAL AND REACTIVITY DESCRIPTOR OF CARISOPRODOL FROM DFT AND MOLECULAR DOCKING APPROACH

Tarun Chaudhary¹, Manoj Kumar Chaudhary^{1,2}, Bhawani Datt Joshi^{3*}

¹Central Department of Physics, Tribhuvan University, Kirtipur, Kathmandu, Nepal

²Department of Physics, University of Lucknow, Lucknow-226007, India

³Department of Physics, Siddhanath Science Campus, Tribhuvan University, Mahendranagar, 10406, Nepal

*Corresponding author: bhawani.joshi@sncs.tu.edu.np, pbdjoshi@gmail.com

(Received: February 05, 2021; Revised: June 01, 2021; Accepted: June 08, 2021)

ABSTRACT

This study aims to investigate the optimized structure and optimized parameters of carisoprodol from the DFT/B3LYP/6-31G(d,p) level of theory. The molecular electrostatic potential (MEP) map signifies that the positive potential across hydrogen of the amine group (NH₂) and the negative potential around the carbonyl groups (C=O). HOMO-LUMO energy gap was found to be 8.1064 eV. The global and local reactivity parameters describe the possible chemical reactive sites in the molecule. The topological analysis of the electron localization function (ELF) and localized orbital locator (LOL) revealed that the charge localization around hydrogen atoms. The hyper-conjugative interaction between donor and acceptor orbital showed that the interaction LP(2) O4 → σ*(O2-C16) plays a vital role in the molecular stability. The molecular docking simulation encircles that the carisoprodol behaves as a good inhibitor with the target protein, Tyrosine-protein kinase ABL.

Keywords: Carisoprodol, Electrostatic potential, Energy gap, Orbital locator, Molecular docking

INTRODUCTION

Carisoprodol (C₁₂H₂₄N₂O₄), chemically known as (RS)-2-[[[(aminocarbonyl)oxy]methyl]-2-methyl pentyl isopropyl carbamate is a centrally acting muscle-skeletal relaxant (Reeves *et al.*, 1999). It is used to treat a craniomandibular disorder, sciatica, lumbago, and other lower back syndromes (Kumar *et al.*, 2017; Horio *et al.*, 2004). Literature reveals that the recent works on carisoprodol were mainly focused on its physical, chemical, and biological properties. Bolattin *et al.* (2016) studied biomolecular interactions of carisoprodol with bovine serum albumin by fluorescence and UV-visible spectroscopy along with a molecular docking approach. Further, the thermal behavior and dynamic fragility in its amorphous state were studied by Diogo *et al.* (2018).

Recently, Liu *et al.* (2020) studied the binding activity of carisoprodol on GABA (Gamma-Aminobutyric Acid) receptor by both docking and molecular dynamics (MD) simulation methods. Chaudhary *et al.* (2021a) performed AIM analysis and investigated vibrational spectra and the nonlinear optical (NLO) properties of the title molecule. However, the structural and spectroscopic properties like calculation of optimized parameters, NBO analysis, HOMO and LUMO energies, MEP, global and local reactivity, the electron localization function (ELF), and the localized orbital locator (LOL) have not been conducted so far. Hence, the present work is mainly concentrated to explore these properties to study the chemical and biological activities of the molecule. The calculations have been performed by using the functional

B3LYP/6-31G (d,p) and the result is closer to the experimental one (Horio *et al.*, 2004).

MATERIALS AND METHODS

The quantum mechanical study of carisoprodol was performed using the Gaussian 09 program package (Frisch *et al.*, 2009). The geometry was optimized through density functional theory (DFT) calculation by employing the functional B3LYP/6-31G(d,p) (Becke, 1993; Parr & Yang, 1989). The GaussView 05 program was used to visualize and interpret the output data of Gaussian 09. It was used to plot HOMO, LUMO, and MEP maps. Furthermore, Multiwfn 3.4.1 (Lu & Chen, 2012) and VMD 1.9.1 (Humphrey *et al.*, 1996) program packages were used for computation and visualization of ELF (electron localization function) and LOL (localized molecular orbital). The molecular docking of carisoprodol has been carried out with AutoDock-Vina software (Trott & Olson, 2010) and ligand-protein interaction has been visualized with bio visualizer software (Studio, 2009).

To determine the chemical reactivity of carisoprodol, molecular electrostatic potential map, the energy of the highest occupied molecular orbital (E_H) and the lowest occupied molecular orbital (E_L), energy gap (E_L-E_H), global reactivity, and local reactivity descriptors have been calculated. The molecular electrostatic potential V(r) (Sjoberg *et al.*, 1990) which is used to generate MEP was calculated using the equation (1).

$$V(r) = \sum_A \frac{Z_A}{|R_A - \vec{r}|} - \int \frac{\rho(r')}{|r' - \vec{r}|} \quad (1)$$

Where, Z_A and $\rho(\vec{r})$ are nuclear charge and electron density respectively.

The chemical potential (μ) of a system is the first-order partial derivatives of energy (E) for the number of electrons (N) at constant external potential V(r).

$$\mu = \left(\frac{\partial E}{\partial N} \right)_{V(r)} = -\chi \quad (2)$$

The words hardness (η) and softness (S) were first introduced by Pearson to check the direction of the acid-base reaction as well as to gain the stability of the product. From the Koopmans theorem, η is half of the energy gap between HOMO and LUMO which signifies to bear the resistance of the system to take or give up electrons. The global hardness which is the inverse of softness is the second-order derivative of energy (E) concerning the number of electrons (N) at constant external potential V(r).

$$\eta = \frac{1}{2} \left(\frac{\partial^2 E}{\partial N^2} \right)_{V(r)} = \frac{1}{2} \left(\frac{\partial \mu}{\partial N} \right)_{V(r)} \quad (3)$$

Electrophilicity index (ω) is introduced by Parr and Pearson (1983) which is a global reactivity descriptor. It is the characteristics of atoms that include the reduction of energy procedure during the absorption of electrons from the donors. The chemical reactivity of the molecule is analyzed in terms of electrophilicity index (ω). It measures the stabilization in energy as the molecule gain external electronic charge from neighboring donor species.

Global reactivity descriptor is used to determine the reactivity of a molecule. Koopman's theorem described the global reactivity parameters like electronegativity (χ), chemical potential (μ), hardness (η), electrophilicity index (ω) and softness (S) are estimated using the equations (4)-(9) (Parr & Pearson, 1983; Joshi, 2016).

$$\chi = -\frac{1}{2}(E_L + E_H) \quad (4)$$

$$\mu = -\chi = \frac{1}{2}(E_L + E_H) \quad (5)$$

$$\eta = \frac{1}{2}(E_L - E_H) \quad (6)$$

$$S = \frac{1}{2\eta} \quad (7)$$

$$\omega = \frac{\mu^2}{2\eta} \quad (8)$$

$$\Delta N_{max} = -\frac{\mu}{\eta} \quad (9)$$

Here, ω measures the stabilization energy after the system gains the extra charge (ΔN) from neighboring molecules and ΔN_{max} is the maximum charge gained by electrophile (Parr *et al.*, 1999). Fukui functions help to predict the particular site for the chemical activity. The high values of

Fukui functions $f(r)$ indicate the high reactivity (Yang & Parr., 1985). The Fukui functions $f_A^+(r)$, $f_A^-(r)$ and $f_A^0(r)$ corresponds to the nucleophilic, electrophilic, and radical attacks respectively. The given Fukui equations for the nucleophilic, electrophilic, and radical attack are:

$$f_A^+(r) = [q_A(N+1) - q_A(N)] \quad (10)$$

$$f_A^-(r) = [q_A(N) - q_A(N-1)] \quad (11)$$

$$f_A^0(r) = \frac{1}{2}[q_A(N+1) - q_A(N-1)] \quad (12)$$

Where, q_A is an atomic charge of the A^{th} atomic site corresponding to neutral (N), anionic (N+1), or cationic (N-1) chemical state of the molecule.

To interpret the charge delocalization in a molecule, NBO analysis had been performed using the same level of theory. The given equation which is based on second-order perturbation theory was used to compute the stabilization energy (E2) between the donor and the acceptor groups (Prajapati *et al.*, 2016; Reed *et al.*, 1988):

$$E(2) = E(i, j) = q_i \frac{F_{ij}^2}{(E_j - E_i)} \quad (13)$$

Where, q_i , E_i , E_j , and F_{ij} are donor orbital occupancy, donor orbital energy, acceptor orbital energy, and off-diagonal elements of the Fock-matrix, respectively.

RESULTS AND DISCUSSION

Geometrical parameters

The geometry of carisoprodol was fully optimized at the DFT-B3LYP level using a 6-31G(d,p) basis set. The optimized structure of carisoprodol is shown in Fig. 1. The comparative study of optimized parameters (bond lengths, bond angles, and dihedral angles) with the geometry of crystal structure (Horio *et al.*, 2004) has been presented in Table 1. Almost all the calculated values are approximately equal to its crystal structure parameters.

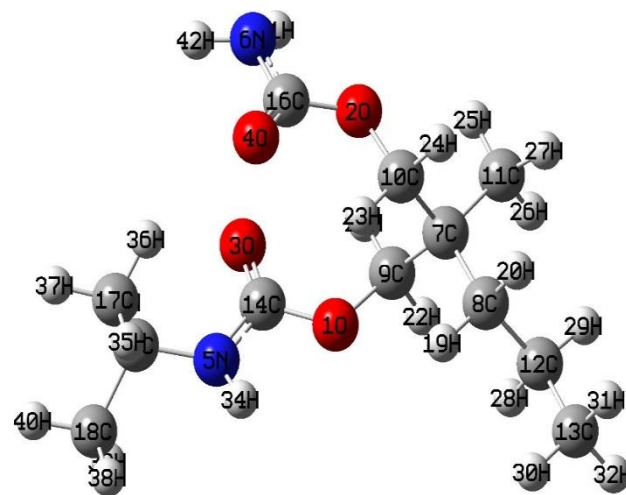


Fig. 1. Optimized structure of carisoprodol

The calculated values of bond lengths N5-H34, N6-H41, and N-H42 are 0.891, 0.966, and 0.779 Å, whereas their respective crystal structure values are 1.011, 1.010, and 1.009 Å. Similarly, the optimized bond angles (C14-N5-H34), (C15-N5-H34), and (C16-N6-H41) are calculated as 116.16°, 118.46° and 116.38°, and the crystal structure values are 113.07°, 107.86° and 119.34°, respectively. The difference in structural parameters is due to the intermolecular hydrogen bonding in solid form. However, this work is based on computational evaluation for a single isolated molecule in the gaseous state.

Molecular electrostatic potential

The molecular electrostatic potential (MEP) map is an important tool to explain the chemical reactivity, hydrogen bonding, and structural activity of different biomolecules including drugs (Joshi *et al.*, 2014). Based on the mapped potential energy surface, the relative polarity of molecule, chemically reactive sites can be predicted. On the MEP, the red surface shows the most electronegative region and the blue surface shows the most positive region.

Table 1. Selected optimized parameters of carisoprodol

Bond length (Å)	Crystal	Calculated	Bond angles (°)	Crystal	Calculated
(O1,C9)	1.448	1.440	(C9,O1,C14)	115.06	116.91
(O1,C14)	1.360	1.369	(C14,N5,C15)	121.70	122.16
(O2,C10)	1.450	1.440	(C14,N5,H34)	113.07	116.16
(O2,C16)	1.343	1.362	(C15,N5,H34)	107.86	118.46
(O3,C14)	1.214	1.221	(C16,N6,H41)	119.34	116.38
(O4,C16)	1.222	1.218	(C16,N6,H42)	115.86	113.88
(N5,C14)	1.379	1.359	(H41,N6,H42)	124.73	115.72
(N5,C15)	1.445	1.465	(O2,C10,C7)	108.71	110.30
(N5,H34)	0.891	1.011	(O2,C10,H23)	107.56	108.72
(N6,C16)	1.348	1.368	(O1,C13,O3)	124.93	124.62
(N6,H41)	0.966	1.010	(O1,C13,N5)	109.66	109.58
(N6,H42)	0.779	1.009	(O3,C13,N5)	125.35	125.78
(C7,C9)	1.550	1.539	(N5,C15,C17)	110.85	111.24
Dihedral Angles (°)	Crystal		Calculated		
(C8,C12,C13,H30)	58.53		59.7365		
(C8,C12,C13,H31)	-50.69		-60.066		
(H28,C12,C13,H31)	177.50		177.8358		
(H29,C12,C13,H31)	66.77		62.1842		
(C18,C15,C17,H35)	63.98		59.0411		
(C18,C15,C17,H36)	178.09		179.0676		
(C18,C15,C17,H37)	-56.33		-60.0656		
(C18,C15,C17,H35)	63.98		59.0411		

Further, the lighter color or almost white surface explains the non-polar nature of molecules. The MEP counter map of carisoprodol is shown in Fig. 2 which demonstrates negative regions over O3 and O4 and positive regions over H34, H41, and H42. The region over oxygen of carbonyl groups, C14=O3 and C16=O4 are almost equal whereas the region over hydrogen (H41 and H42) of primary amine are comparatively more positive than the region over hydrogen of secondary amine (H34). The molecular docking analysis shows that the atoms O1, O2,

O3, and O4 actively participated in hydrogen bonding with the protein during the ligand-protein interaction.

HOMO-LUMO analysis

The chemical stability of molecules depends upon the energy of the highest occupied molecular orbital (HOMO) and the lowest unoccupied molecular orbital (LUMO). The orbital energy HOMO (E_H) acts as the electron donor and the orbital energy LUMO (E_L) acts as the electron acceptor and their energy gap (E_L-E_H) determines the

chemical reactivity of the molecule (Chaudhary *et al.*, 2021b; Joshi *et al.*, 2018). The probability of electronic transition activity increases with the increase in the energy gap and vice-versa (Fukui, 1982). To understand the chemical stability of carisoprodol, time-dependent DFT calculations have been performed employing the B3LYP/6-31G (d, p) level of theory. The energy gap for carisoprodol is obtained as 8.1064 eV. The HOMO-LUMO plot of the molecule shown in Fig. 3 signifies that the electron density in HOMO is concentrated on O1, C14=O3, and N5H34 whereas the charge diverges on C16=O4 and N6H2 in LUMO.

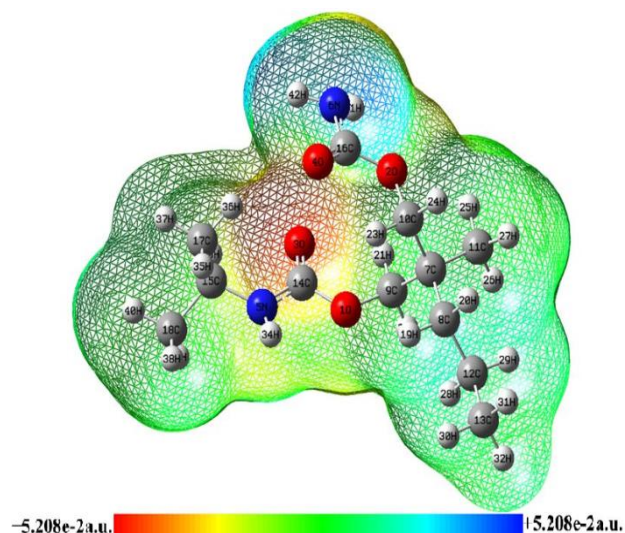


Fig. 2. Molecular electrostatic potential map of carisoprodol

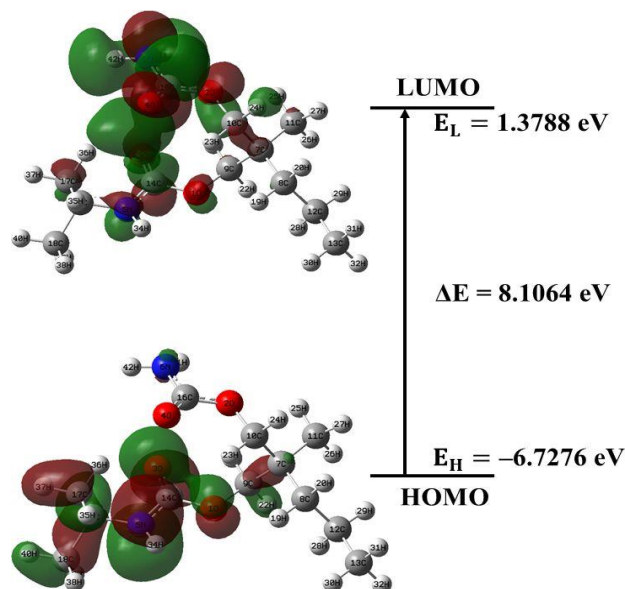


Fig. 3. HOMO and LUMO plot of carisoprodol

Global reactivity

The high value of μ and ω indicates good electrophilic behavior and low-value μ and ω indicates nucleophilic behavior of the molecules, respectively (Chaudhary *et al.*, 2020; Joshi, 2017). The electrophilicity index (ω) and softness (S) describes the stability of the molecules. The chemical activity increases with a decrease of the energy gap ($E_L - E_H$) and vice-versa. The values of frontier molecular orbitals (FMOs) energies with their energy gap ($E_L - E_H$) and parameters; χ , μ , η , ω and S are illustrated in Table 2.

Table 2. Calculated E_H , E_L energy, band gap ($E_L - E_H$), chemical potential (μ), electronegativity (χ), global hardness (η), global softness (S), and global electrophilicity index (ω) for carisoprodol

E_H (eV)	E_L (eV)	$E_L - E_H$ (eV)	χ (eV)	μ (eV)	η (eV)	S (eV) ⁻¹	ω (eV)
-6.7276	1.3788	8.1064	2.6744	-2.6744	4.0532	0.1234	0.8823

Local reactivity

To explore the quantitative reactive site, the local reactivity descriptors parameters have been calculated. Fukui functions help to predict the particular site for the chemical reactivity. To investigate the particular sites for nucleophilic and electrophilic attack more precisely, we have performed Fukui function analysis. The local reactivity descriptors of the title molecule have been presented the Table 3. The analysis of local reactivity descriptors shows that the most probable nucleophilic and electrophilic sites of the molecule are C16 and C14, respectively.

Topological analysis (ELF and LOL)

The density-based description of chemical bonding, the electron localization function (ELF), and the localized

orbital locator (LOL) were introduced in literature (Becke & Edgecombe, 1990; Schmider & Becke, 2002). The ELF and LOL exhibit similar interpretations based on kinetic energy density in which, electron pair density is considered in ELF, and gradients of localized orbitals were recognized in LOL (Schmider & Becke, 2000; Rizwana *et al.*, 2020). The values of ELF and LOL fall within the range 0-1, whereas values greater than 0.5 indicate the region of localized electrons and the values smaller than 0.5 indicate the region for delocalized electrons. The value of ELF is high if Pauli's repulsion is high and vice versa. The localized electrons represent the atomic shells, chemical bonds, and lone pair electrons (Abraham *et al.*, 2018).

The Topological analysis of ELF and LOL of the title molecule based on covalent bonds has been performed

using Multiwfn software. The ELF and LOL map of electrons are presented in Figs. 4(a) and 4(b), respectively. The region around the hydrogen atom is depicted by the red region (high LOL values) which is due to maximum Pauli repulsion. The red region around O2 and N5 indicates the presence of localized electron lone pairs. Similarly, the covalent bond region between carbon atoms is characterized by red color showing a high degree of electron localization in that place. On the other hand, the blue ring (low LOL values) region is obtained around the nucleus of O2, C7, C12, C15, and N5 which is the region between the inner shell and valence shell showing a very low degree of electron localization in that zones.

Table 3. Calculated local reactivity properties of the selected atoms using Hirshfeld [B3LYP/6-31G (d,p)] derived charges of carisoprodol

Site	f_k^+	Site	f_k^-	Site	f_k^0
N5	0.71809	C14	0.45364	C16	0.484545
N6	0.54164	C16	0.4298	C14	0.462195
O4	0.47303	C15	-0.03689	C15	-0.03287
O3	0.44081	C7	-0.05088	C7	-0.04419
C17	0.39192	C10	-0.06599	C10	-0.05063
C18	0.36003	C9	-0.06719	C9	-0.05111
O1	0.35283	C12	-0.24017	N5	-0.15244
C11	0.34618	C8	-0.24339	C12	-0.2241
C13	0.33921	O2	-0.28615	C8	-0.22981
O2	0.31333	O1	-0.29079	O1	-0.26587
C8	0.23454	O4	-0.32017	O4	-0.26713
C12	0.23021	O3	-0.33656	O2	-0.28333
C9	0.06022	N5	-0.34209	O3	-0.28569
C7	0.05691	C13	-0.34877	C17	-0.32884
C10	0.05691	C18	-0.3557	C18	-0.33597
C15	0.02592	C11	-0.35806	C13	-0.3382
C16	-0.49487	C17	-0.36145	C11	-0.34277
C14	-0.51843	N6	-0.44489	N6	-0.38874

Natural bond orbital (NBO) analysis

NBO analysis is the fundamental tool to interpret the delocalization of charge from donor Lewis type (occupied) orbitals to acceptor Lewis type (unoccupied) orbitals or lone pair to acceptor orbital, within the molecule, to check the stability of the molecular system (Chaudhary *et al.*, 2021c). The stabilization energy $E(2)$ is determined by the second-order perturbation theory. Higher the value of $E(2)$, the stronger the interaction between donor and acceptor orbital, and vice versa. For carisoprodol, the NBO analysis has been carried out by B3LYP/6-31G(d,p) and the selected hyper-conjugative

interaction of stabilization energy $E(2)$ greater than 5 kcal/mol is presented in Table 4.

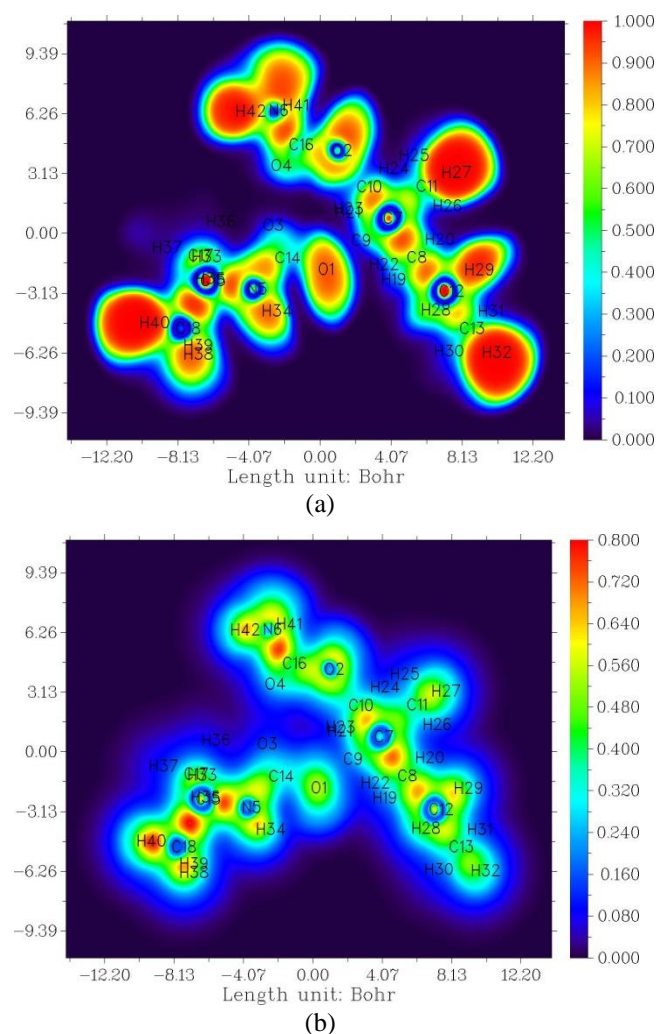


Fig. 4. ELF color-filled map of carisoprodol (a) and LOL color-filled map of carisoprodol (b)

In the carisoprodol the donor orbitals are generally associated with O1, O2, O3, O4, N5, and N6 whereas the acceptor orbitals are mainly concentrated across (O3-C14), (O2-C16), and (O4-C16). The transition from $LP(2)O1 \rightarrow \sigma^*(O3-C14)/\pi^*(O3-C14)$ stabilizes the molecule with respected energies 6.12/19.32 kcal/mol. Similarly, the strongest interaction $LP(2)O4 \rightarrow \sigma^*(O2-C16)$ gives the highest stabilization energy 33.19 kcal/mol. Moreover, the transition which participates for the stability of a molecule is $LP(2)O3 \rightarrow \sigma^*(O1-C14)$, $LP(1)N5 \rightarrow \pi^*(O3-C14)$, $LP(2)O2 \rightarrow \pi^*(O4-C16)$, and $LP(2)O4 \rightarrow \sigma^*(N6-C16)$, with the corresponding stabilization energy 33.02, 26.12, 23.95, and 22.37 kcal/mol. Also, the overlapping of $\sigma(N6-H42) \rightarrow \sigma^*(O2-C16)$ and $LP(1)N5 \rightarrow \sigma^*(O3-C14)$ stabilizes the molecule to some extent with interaction energy 5.05 and 9.01 kcal/mol, respectively.

Molecular docking of carisoprodol

The molecular docking simulation is a very popular tool to study ligand-protein interaction and to investigate the insight properties of the drug molecule (Chaudhary *et al.*, 2021d). In the present work, to study the biological activities of carisoprodol (ligand), the docking analysis has been conducted by using AutoDock-Vina software.

The target protein, Tyrosine-protein kinase ABL has been predicted with the help of Swiss Target Prediction (Gfeller *et al.*, 2014). It is a human protein that is known to be essential for transforming activity (Buchdunger *et al.*, 1996). The PDB structure of this protein (1awo) has been downloaded from the RSCB PDB data bank (Rose *et al.*, 2010). Further, the Ramchandran Plots of the protein have been presented in Fig. 5.

Table 4. Second-order perturbation theory analysis of Fock matrix in NBO basis of carisoprodol

Donor NBO(i)	ED (i)/e	Acceptor NBO(j)	ED(j)/e	E(2) ^a kcal/mol	E(j)-E(i) ^b a.u.	F(i,j) ^c a.u.
σ (N6-H42)	1.98354	σ^* (O2-C16)	0.10895	5.05	1.02	0.065
LP(1)O1	1.96128	σ^* (O3-C14)	0.13671	6.99	0.97	0.075
LP(2)O1	1.83349	σ^* (O3-C14)	0.13671	6.12	0.73	0.060
LP(2)O1	1.83349	π^* (O3-C14)	0.27031	19.32	0.51	0.091
LP(2)O2	1.82575	π^* (O4-C16)	0.26555	23.95	0.49	0.099
LP(2)O3	1.82617	σ^* (O1-C14)	0.10898	33.02	0.60	0.128
LP(2)O3	1.82617	σ^* (N5-C14)	0.06741	22.12	0.73	0.116
LP(2)O4	1.83134	σ^* (O2-C16)	0.10895	33.19	0.61	0.129
LP(2)O4	1.83134	σ^* (N6-C16)	0.06426	22.37	0.70	0.115
LP(1)N5	1.73537	σ^* (O3-C14)	0.13671	9.01	0.67	0.072
LP(1)N5	1.73537	π^* (O3-C14)	0.27031	26.12	0.45	0.097
LP(1)N5	1.73537	σ^* (C15-C17)	0.02192	6.20	0.64	0.060
LP(1)N6	1.79977	σ^* (O4-C16)	0.11244	8.03	0.74	0.070
LP(1)N6	1.79977	π^* (O4-C16)	0.26555	20.26	0.46	0.088

^aE(2) means the energy of hyper conjugative interaction (stabilization energy); ^bEnergy difference between the donor (i) and acceptor (j) NBO orbitals and ^cF(i,j) is the Fock matrix element between i and j NBO orbitals

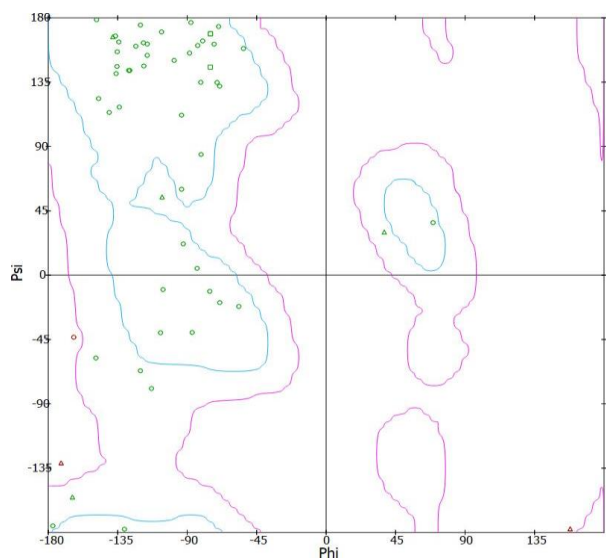


Fig. 5. Ramchandran plot of 1awo

The regions inside the first blue line indicate allowed ones and those outside it indicate disallowed regions, respectively. Hence, the maximum number of residues lies within the allowed region. The optimized structure of carisoprodol (ligand) obtained at B3LYP/6-31G(d,p) has been used for the docking analysis. The protein (receptor) was prepared by removing water molecules and co-crystallized ligand from the protein and further, the polar hydrogen and Kollman charges were added. The grid box of size 60 Å × 60 Å × 60 Å has been used for studying the binding activities.

The discovery studio was used for the visualization of ligand-protein interaction. The ligand-protein interaction and LiGPLOT are shown in Figs. 6(a) and 6(b). The binding affinity, bond length, bonded residues, and inhibition constant of the docked complex of carisoprodol and 1awo have been presented in Table 5. The atoms O1, O2, O3, and O4 form six hydrogen bonds with the amino acids SER75, GLY76, ASN78, THR79, THR79, and

THR79. The binding energy of docked structure of the investigated molecule with the protein was found to be -5 kcal/mol. Hence, carisoprodol shows strong binding activity with the protein 1wao.

Table 5. The docking parameters of docked structure of carisoprodol and 1wao

Protein	PDB code	Binding affinity (kcal/mol)	Bond length(Å)	Bonded Residues	Types of H-bond	Inhibition constant (µM)
Tyrosine-protein kinase ABL	1awo	-5.0	2.7604	SER75	H-bond	215.16
			2.8959	GLY76	H-bond	
			2.3335	ASN78	H-bond	
			2.3037	THR79	H-bond	
			2.2572	THR79	H-bond	
			2.7032	THR79	H-bond	

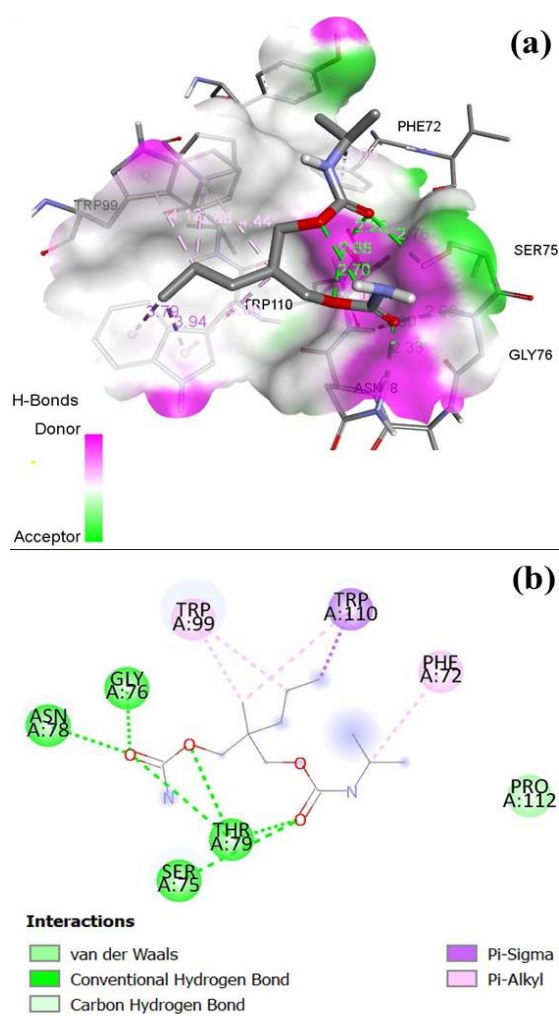


Fig. 6. (a) Docking of carisoprodol with 1wao and (b) LIGPLOT of docking of carisoprodol with 1wao

CONCLUSION

The optimized geometrical parameters and crystal geometrical parameters of carisoprodol were almost in

resonance. The energy gap between HOMO and LUMO was found to be 8.1064 eV. Due to the high value of Fukai functions, the nucleophilic and electrophilic sites are predicted as C16 and C14, respectively. The molecular electrostatic potential map explorers are the negative and positive potentials associated with the carbonyl and amine groups, respectively. ELF and LOL topological analysis signifies that most of the localized electrons were predicted around hydrogen, oxygen, nitrogen, and between carbon atoms.

Further, the NBO analysis demonstrates the intramolecular charge transfer between lone pair LP(2)O4 and $\sigma^*(O2-C16)$, which contribute the highest value of stabilization energy 33.19 kcal/mol. The molecular docking simulation revealed that the carisoprodol strongly binds with the protein 1wao. Also, the oxygen atom of all carbonyl groups actively participated in hydrogen bonding to form a complex.

ACKNOWLEDGEMENT

Authors sincerely acknowledge to Prof. Poonam Tandon, HOD Physics and Dean Student Welfare, University of Lucknow, India for providing software facilities including Gaussian 09 as well as sharing research ideas during the project.

REFERENCES

- Abraham, C. S., Prasana, J. C., Muthu, S., & Raja, M. (2018). Quantum computational studies, spectroscopic (FT-IR, FT-Raman, and UV-Vis) profiling, natural hybrid orbital, and molecular docking analysis on 2, 4 Dibromoaniline. *Journal of Molecular Structure*, 1160, 393-405.
- Becke, A. D. (1993). A new mixing of Hartree-Fock and local density-functional theories. *The Journal of Chemical Physics*, 98(2), 1372-1377.
- Becke, A. D., & Edgecombe, K. E. (1990). A simple measure of electron localization in atomic and

- molecular systems. *The Journal of Chemical Physics*, 92(9), 5397-5403.
- Bolattin, M. B., Nandibewoor, S. T., Joshi, S. D., Dixit, S. R., & Chimataadar, S. A. (2016). Interaction between carisoprodol and bovine serum albumin and effect of β -cyclodextrin on binding: insights from molecular docking and spectroscopic techniques. *RSC Advances*, 6(68), 63463-63471.
- Buchdunger, E., Zimmermann, J., Mett, H., Meyer, T., Müller, M., Druker, B. J., & Lydon, N. B. (1996). Inhibition of the Abl protein-tyrosine kinase in vitro and in vivo by a 2-phenylaminopyrimidine derivative. *Cancer Research*, 56(1), 100-104.
- Chaudhary, M. K., Chaudhary, T., & Joshi, B. D. (2021a). Simulated spectra (IR and Raman), NLO, AIM, and molecular docking of carisoprodol from DFT approach. *Bibechana*, 18(1), 48-57.
- Chaudhary, M. K., Karthick, T., Joshi, B. D., Prajapati, P., de Santana, M. S. A., Ayala, A. P., Reeda, V. S. J., & Tandon, P. (2021b). Molecular structure and quantum descriptors of cefradine by using vibrational spectroscopy (IR and Raman), NBO, AIM, chemical reactivity, and molecular docking. *Spectrochimica Acta Part A: Molecular and Biomolecular Spectroscopy*, 246, 118976. <https://doi.org/10.1016/j.saa.2020.118976>
- Chaudhary, M. K., Prajapati, P., Srivastava, K., Silva, K. F., Joshi, B. D., Tandon, P., & Ayala, A. P. (2021c). Molecular interactions and vibrational properties of ribobenzazole: Insights from quantum chemical calculation and spectroscopic methods. *Journal of Molecular Structure*, 1230, 129889. <https://doi.org/10.1016/j.molstruc.2021.129889>
- Chaudhary, M. K., Srivastava, A., Singh, K. K., Tandon, P., & Joshi, B. D. (2020). Computational evaluation on molecular stability, reactivity, and drug potential of frovatriptan from DFT and molecular docking approach. *Computational and Theoretical Chemistry*, 1191, 113031. <https://doi.org/10.1016/j.comptc.2020.113031>
- Chaudhary, T., Chaudhary, M. K., Joshi, B. D., de Santana, M. S. A., & Ayala, A. P. (2021d). Spectroscopic (FT-IR, Raman) analysis and computational study on conformational geometry, AIM and biological activity of cephalixin from DFT and molecular docking approach. *Journal of Molecular Structure*, 1240, 130594. <https://doi.org/10.1016/j.molstruc.2021.130594>
- Diogo, H. P., Ramos, J. J. M., & Piedade, M. F. M. (2018). Thermal behavior and dynamic fragility in amorphous carisoprodol. Correlation between the dynamic and thermodynamic fragilities. *Thermochimica Acta*, 663, 99-109.
- Frisch, M. J., Trucks, G. W., Schlegel, H. B., Scuseria, G. E., Cheeseman, J. R., Robb, M. A., & Fox, D. J., (2009). GAUSSIAN 09, revision, Gaussian, Inc., Wallingford CT.
- Fukui, K. (1982). Role of frontier orbitals in chemical reactions. *Science*, 218(4574), 747-754.
- Gfeller, D., Grosdidier, A., Wirth, M., Daina, A., Michielin, O., & Zoete, V. (2014). Swiss target prediction: a web server for target prediction of bioactive small molecules. *Nucleic Acids Research*, 42(1), W32-W38
- Horio, K., Tanaka, R., Akama, H., Haramura, M., Tanaka, A., Akimoto, T., & Hirayama, N. (2004). Crystal structure of carisoprodol. *Analytical Sciences: X-ray Structure Analysis Online*, 20, x43-x44.
- Humphrey, W., Dalke, A., & Schulten, K. (1996). VMD: visual molecular dynamics. *Journal of Molecular Graphics*, 14(1), 33-38.
- Joshi, B. D. (2016). Chemical reactivity, dipole moment and first hyperpolarizability of aristolochic acid I. *Journal of Institute of Science and Technology*, 21(1), 1-9.
- Joshi, B. D. (2017). Structural, electronic and vibrational study of 4, 6-dichloro-5-methyl pyrimidine: A DFT approach. *Journal of Institute of Science and Technology*, 22(1), 51-60.
- Joshi, B. D., Khadka, J. B., & Bhatt, A. (2018). Structure, electronic and vibrational study of 7-methyl-2, 3-dihydro-(1, 3) thiazolo (3, 2-A) pyrimidine-5-one by using density functional theory. *Journal of Institute of Science and Technology*, 22(2), 1-11.
- Joshi, B. D., Mishra, R., Tandon, P., Oliveira, A. C., & Ayala, A. P. (2014). Quantum chemical studies of structural, vibrational, NBO and hyperpolarizability of ondansetron hydrochloride. *Journal of Molecular Structure*, 1058, 31-40.
- Kumar, K. A., Lakshmi pathi, V. S., Meenakshi, S., & Balakrishnan, M. H. (2017). Synthesis and characterization of potential impurity of muscle relaxant drug carisoprodol. *Journal Chemistry and Chemical Sciences*, 7(4), 352-360.
- Liu, J., Huang, R., & Claudio, M. (2020). Determining the binding site of carisoprodol on GABAA receptor. <https://hdl.handle.net/20.500.12503/30337>
- Lu, T., & Chen, F. (2012). Multiwfn: a multifunctional wave function analyzer. *Journal of Computational Chemistry*, 33(5), 580-592.

- Parr, R. G., & Pearson, R. G., (1983). Absolute hardness: companion parameter to absolute electronegativity. *Journal of the American Chemical Society*, 105(26), 7512-7516.
- Parr, R. G., & Yang, W. (1989). *Density-functional theory of atoms and molecules*. Oxford University Press, New York Oxford.
<https://doi.org/10.1002/qua.560470107>
- Parr, R. G., Szentpály, L. V., & Liu, S. (1999). Electrophilicity index. *Journal of the American Chemical Society*, 121(9), 1922-1924.
- Prajapati, P., Pandey, J., Shimpi, M. R., Srivastava, A., Tandon, P., Velaga, S. P., & Sinha, K. (2016). Combined spectroscopic and quantum chemical studies of ezetimibe. *Journal of Molecular Structure*, 1125, 193-203.
- Reed, A. E., Curtiss, L. A., & Weinhold, F. (1988). Intermolecular interactions from a natural bond orbital, donor-acceptor viewpoint. *Chemical Reviews*, 88(6), 899-926.
- Reeves, R. R., Carter, O. S., Pinkofsky, H. B., Struve, F. A., & Bennett, D. M. (1999). Carisoprodol (Soma) abuse potential and physician unawareness. *Journal of Addictive Diseases*, 18(2), 51-56.
- Rizwana, B. F., Prasana, J. C., Muthu, S., & Abraham, C. S. (2020). Vibrational spectroscopy, reactive site analysis and molecular docking studies on 2-[(2-amino-6-oxo-6, 9-dihydro-3H-purin-9-yl) methoxy]-3-hydroxypropyl (2S)-2-amino-3-methyl butanoate. *Journal of Molecular Structure*, 1202, 127274.
- Rose, P. W., Beran, B., Bi, C., Bluhm, W. F., Dimitropoulos, D., Goodsell, D. S., Prlic, A., Quesada, M., Quinn, G. B., Westbrook, J. D., Young, J., Yukich, B., Zardecki, C., Berman, H. M., & Bourne, P. E. (2010). The RCSB protein data bank: redesigned website and web services. *Nucleic Acids Research*, 39(sup. 1 1), D392-D401.
- Schmider, H. L., & Becke, A. D. (2000). Chemical content of the kinetic energy density. *Journal of Molecular Structure: Theochem*, 527(1-3), 51-61.
- Schmider, H. L., & Becke, A. D. (2002). Two functions of the density matrix and their relation to the chemical bond. *The Journal of Chemical Physics*, 116(8), 3184-3193.
- Sjoberg, P., Murray, J. S., Brinck, T., & Politzer, P. (1990). Average local ionization energies on the molecular surfaces of aromatic systems as guides to chemical reactivity. *Canadian Journal of Chemistry*, 68(8), 1440-1443.
- Studio, D. (2009). *Version 2.5 guide*. San Diego, CA: Accelrys Inc., p. 92121.
- Trott, O., & Olson, A. J., (2010). AutoDock Vina: Improving the speed and accuracy of docking with a new scoring function, efficient optimization, and multithreading. *Journal of Computational Chemistry*, 31, 455-461.
- Yang, W., & Parr, R. G. (1985). Hardness, softness, and the Fukui function in the electronic theory of metals and catalysis. *Proceedings of the National Academy of Sciences*, 82(20), 6723-6726.